LBL-25201
Preprint

Lawrence Berkeley Laboratory
UNIVERSITY OF CALIFORNIA

RECEIVED
LAWRENCE
BERKELEY LABORATORY

JUN 9 1988

LIBRARY AND
DOCUMENTS SECTION

Submitted to Physical Review C

Total Projectile Kinetic Energy Scaling in Energetic Nucleus-Nucleus Collisions

W. Loveland, Z. Xu, C. Casey, K. Aleklett, J.O. Lilijenzin,
D. Lee, and G.T. Seaborg

April 1988

TWO-WEEK LOAN COPY
This is a Library Circulating Copy
which may be borrowed for two weeks.

NUCLEAR SCIENCE DIVISION

Prepared for the U.S. Department of Energy under Contract Number DE-AC03-76SF00098.

LBL-25201 c.2

DISCLAIMER

This document was prepared as an account of work sponsored by the United States Government. While this document is believed to contain correct information, neither the United States Government nor any agency thereof, nor the Regents of the University of California, nor any of their employees, makes any warranty, express or implied, or assumes any legal responsibility for the accuracy, completeness, or usefulness of any information, apparatus, product, or process disclosed, or represents that its use would not infringe privately owned rights. Reference herein to any specific commercial product, process, or service by its trade name, trademark, manufacturer, or otherwise, does not necessarily constitute or imply its endorsement, recommendation, or favoring by the United States Government or any agency thereof, or the Regents of the University of California. The views and opinions of authors expressed herein do not necessarily state or reflect those of the United States Government or any agency thereof or the Regents of the University of California.

TOTAL PROJECTILE KINETIC ENERGY SCALING IN ENERGETIC NUCLEUS-NUCLEUS COLLISIONS

W. Loveland, Z. Xu, C. Casey

Dept. of Chemistry,
Oregon State University
Corvallis, OR 97331

K. Aleklett

Studsvik Neutron Research Laboratory
S-61182 Nykoping, Sweden

J. O. Lilijenzin

Dept. of Chemistry
University of Oslo
0315 Oslo 3, Norway

Diana Lee and G. T. Seaborg

Nuclear Science Division
Lawrence Berkeley Laboratory
University of California
Berkeley, CA 94720

This work was supported by the Director, Office of Energy Research, Division of Nuclear Physics of the Office of High Energy and Nuclear Physics of the U.S. Department of Energy under Contract No. DE-AC03-76SF00098.

TOTAL PROJECTILE KINETIC ENERGY SCALING IN ENERGETIC NUCLEUS-NUCLEUS COLLISIONS

W. Loveland, Z. Xu, C. Casey

Dept. of Chemistry,
Oregon State University
Corvallis, OR 97331

K. Aleklett

Studsvik Neutron Research Laboratory
S-61182 Nykoping, Sweden

J. O. Liljenzin

Dept. of Chemistry
University of Oslo
0315 Oslo 3, Norway

Diana Lee and G.T. Seaborg

Nuclear Science Division
Lawrence Berkeley Laboratory
Berkeley, CA 94720

ABSTRACT

The target fragment production cross sections have been measured for the reaction of 150 MeV/nucleon ^{139}La with ^{197}Au. From these cross sections, the fragment isobaric yields were deduced. The resulting isobaric yield distribution is very similar to that observed for reactions in which limiting fragmentation is occurring (such as the reaction of 8 GeV ^{20}Ne with ^{197}Au) and unlike that observed with projectiles of similar velocity. This apparent extreme example of total projectile kinetic energy scaling is compared to predictions of the intra-nuclear cascade model.

PACS Numbers 25.70.Np

I. Introduction

In studies of target fragmentation[1)] induced by lighter heavy ions, one finds the single particle inclusive target fragment production cross sections become energy independent at projectile energies of approximately 10 GeV (limiting fragmentation[2)]). Furthermore one finds[1)] that it is the kinetic energy of the projectile rather than its velocity or rapidity that is the proper scaling variable with respect to limiting fragmentation. In this paper, we present the results of a study of the reaction of 150 MeV/nucleon (20.9 GeV) ^{139}La with ^{197}Au in which it appears that the concept of total projectile kinetic energy scaling is valid in perhaps what is the most extreme application of this concept.

II. Experimental Methods

The target fragment production cross sections from the interaction of 150 MeV/nucleon ^{139}La with ^{197}Au were determined using radiochemical techniques similar to those used previously[3)]. Gold foils surrounded by carbon catcher foils were irradiated with an external beam of 150 MeV/nucleon ^{139}La from the LBL Bevalac. The beam intensities were measured using an Ar-CO_2 ion chamber that had been calibrated by direct counting of the beam using a plastic scintillator. Two separate irradiations were performed in which 2.7×10^{11} ions passed through the target foils in periods of 1710 and 3364 minutes, respectively. In the first irradiation, two gold target stacks were employed. In the first stack, the gold target (thickness 123.6 mg/cm^2) was surrounded by 18.3 mg/cm^2 carbon catcher foils. The gold target from this stack was processed radiochemically as described below. The second stack consisted of a gold foil of thickness 134.9 mg/cm^2 surrounded by 20 mg/cm^2 carbon catcher foils and was counted without chemical processing. In the second irradiation, a gold target of thickness 250.3 mg/cm^2 surrounded by 35 mg/cm^2 carbon catcher foils was used.

The gold target foil which was processed radiochemically was dissolved in aqua regia and subjected to a standard radiochemical procedure[4]. This procedure yielded seven chemical fractions (in the language of ref. 4,a iodine-bromine fraction, a superheavy fraction, a lead fraction, a uranium fraction, a lanthanide fraction, a thorium fraction, and a gold fraction.) These chemical fractions were assayed along with the unseparated foils by off-line gamma-ray spectroscopy[5]. Corrections for the chemical yields of the separations and for the lack of processing of the catcher foils in the chemical separations were determined using the activities in the unseparated foils. The chemical fractions contained very few radionuclides not seen in the unseparated foils, but the resulting gamma ray spectra contained fewer interfering radionuclides and thus the accuracy and precision of the determination of the radionuclide activities was improved.

Gamma ray spectroscopy began within a few hours after the end of the irradiation and continued for a period of approximately two months. The activity levels in the catcher foils were too low to allow measurement of target fragment recoil properties. These catcher foils were combined with the Au target foils during gamma ray spectroscopy. Formation cross sections for the production of individual radionuclides were calculated using techniques that have been described previously[5].

No corrections were made for the effect of secondary particle induced reactions upon the measured cross sections. Studies[3] made of the interaction of 8.0 GeV ^{20}Ne with a 242.0 mg/cm^2 gold target found a negligible contribution to the yield of most products due to these processes. However, because of the possibility of occurrence of secondary induced reactions, we shall regard the measured production cross sections for near target residues to be upper limits for such cross sections.

III. Experimental Results

The measured fragment production cross sections are shown in Table I. Most noteworthy amongst the nuclidic production cross sections (or upper limits) is the cross section for ^{196}Au, which is 765 ± 48 mb. This very large value for the cross section (or its upper limit) makes one consider whether non-nuclear processes, such as electromagnetic dissociation are contributing to the value of this cross section. Mercier, et al.[6] have pointed out that the cross section for the ^{197}Au(relativistic heavy ion,X) ^{196}Au reaction can be written as the sum of contributions from nuclear and electromagnetic processes

$$\sigma_{TOTAL} = \sigma_{NUCL} + \sigma_{ED} \tag{1}$$

They further point out that the nuclear part of the cross section can be parameterized as

$$\sigma_{NUCL} = \sigma_0 b_c \ (1+aA_p^{2/3}) \tag{2}$$

where b_c is given by

$$b_c = 1.34 \ [A_p^{1/3}+A_t^{1/3}-0.75(A_p^{-1/3}+A_t^{-1/3})] \text{ fm} \tag{3}$$

A_t and A_p are the target and projectile mass numbers while σ_0 and a are constants to be determined. From fitting the data in ref[6], we estimate σ_0=7.889 and a=0.0671. This allows us to calculate a value of σ_{NUCL} of 318 mb, giving σ_{ED}=765-318 = 447 mb. That upper limit value is significantly less than one would calculate for σ_{ED} from modern theories. For example, Winther and Alder[7] have shown that the cross section for exciting the giant dipole resonance in a nucleus with atomic and neutron numbers of Z_2 and N_2, respectively by relativistic heavy ions (Z_1, A_1) moving with velocity β(=v/c) is given as

$$\sigma_{E1} = 1.04 \ (\frac{Z_1 e^2}{h\beta c}) \ \frac{N_2 Z_2}{A_2^{1/3}} \ [g_1(\xi(R))+(1-\beta^2)g_0(\xi(R))] \text{ fm}^2 \tag{4}$$

where

$$\xi(R) = \left(\frac{0.4}{\beta}\right)(1-\beta^2)R_{fm} \tag{5}$$

and R_{fm} is the sum of the radii of the colliding nuclei in fm. The functions $g_n(x)$ are given as

$$g_0(x) = \pi$$
$$g_1(x) = \pi \ln\left(\left(\frac{\alpha}{x}\right)^2+1\right) \tag{6}$$

where α=0.681085. Using the formalism of Winther and Alder and $R=1.2A^{1/3}$ fm, we calculate σ_{ED} for 150 A MeV ^{139}La + ^{197}Au to be 4456 mb, an overestimate of an order of magnitude compared to the cross section (or upper limit) for electromagnetic dissociation deduced above. (We assume that all the giant dipole resonance (E*=13.8 MeV) decays producing ^{196}Au by neutron emission). It should be pointed out that the calculated value of σ_{ED} for the reaction of 8 GeV ^{20}Ne + ^{197}Au is 50 mb, in good agreement with the measured value[3] of σ_{TOT} ($\simeq$174+25 mb) - σ_{NUCL}($\sim$118 mb). Thus it appears that the theory of Winther and Alder overestimates the electromagnetic dissociation cross section for high Z projectiles.

In Figure 1, we show the ratio of the cross sections of "independent yield" nuclides measured in this work to the cross sections for the same nuclides measured for the interaction of 8 GeV ^{20}Ne with ^{197}Au[3]. (By the term "independent yield" nuclides, we refer to shielded nuclides, quasi-shielded nuclides and nuclides whose production by precursor decay is not significant). While the number of nuclidic cross sections that

are compared is not large, the values of the cross sections ratios seem reasonably constant at a value of 1.65±0.12. This is suggestive that the target fragment yields from the reaction of 150 MeV/nucleon (20.8 GeV) ^{139}La with ^{19}Au are similar to those observed in cases where limiting fragmentation is occurring. (It has been shown previously[8], that the target fragment production cross sections are independent of bombarding energy for total projectile energies above 8 GeV).

Comparisons of the formation cross sections for common, independent yield fragments from various reactions utilize only a fraction of the available experimental data for each target-projectile system. To more fully utilize the available data, we have deduced mass-yield (isobaric yield) distributions from the measured formation cross sections. The method employed in this estimation procedure has been discussed previously.[3]

The measured nuclidic formation cross sections were placed in eight groups according to mass number. These cross sections were corrected for precursor beta decay, where necessary, by assuming that the independent yield cross sections for a given species, $\sigma(Z,A)$, can be expressed as a histogram that lies along a Gaussian curve.

$$\sigma(Z,A) = \sigma(A)[2\pi C_Z^2(a)]^{-1/2} \exp[\frac{-(Z-Z_{mp})^2}{2C_Z^2(A)}] \qquad (7)$$

where $C_Z(A)$ is the Gaussian width parameter for mass number A and $Z_{mp}(A)$ is the most probable atomic number for that A. Using this assumption and the further assumption that $\sigma(A)$ varies slowly and smoothly as a function of A (allowing data from adjacent isobars to be combined in determining $Z_{mp}(A)$ and $C_Z(A)$), one can use the laws of radioactive decay to iteratively correct the measured cumulative formation cross sections for precursor decay.

Within each of the eight groups, the data were fit to a Gaussian-shaped independent yield distribution. The width parameter was found to be constant over a given range in A while the center of the charge distribution were adequately represented by linear functions in A over a limited range in A although we expect $Z_{mp}(A)$ to be non-linear. (Only nuclides with well-characterized beta-decay precursors and cases where both members of an isomeric pair were included in the analysis). The nuclidic groupings along with the centers and widths of the Gaussian distributions are given in Table II. The independent yield distributions estimated from the measured formation cross sections are shown in Figure 2.

The isobaric yield distribution obtained from integration of the estimated independent yield distributions is shown in Figure 3. The error bars on the integrated data points reflect only the uncertainties due to counting statistics and do not take into account any uncertainties due to lack of knowledge of the absolute beam intensity (estimated to be approximately 15%), contributions due to secondary reactions (possibly as large as 10%) or those introduced in the charge distribution fitting process. Morrissey et al.[3] have suggested that individual isobaric yields may have systematic uncertainties, due to the fitting process, of approximately 25%. The uncertainties in the isobaric yields are dominated by the latter source of error, with the typical uncertainty being approximately 30%. Also shown as smooth curves in Figure 3 are the isobaric yield distributions for the interaction of roughly equivalent velocity protons[9] and ^{12}C [10] ions with ^{194}Au as well as the mass-yield distribution for 8 GeV ^{20}Ne + ^{197}Au[3]. The latter distribution, as noted above, is taken as representative of the distribution which would result from the interaction of 21 GeV ^{20}Ne (equivalent total projectile energy as 20.8 GeV ^{139}La) since target

fragmentation has been found previously[8] to be limiting with respect to mass yields for light ion projectiles with 7.6 GeV ^{20}Ne + ^{197}Au. The similarity between the isobaric yield distributions for the La + Au and Ne + Au and the lack of similarity between the La + Au distribution and those involving roughly equivalent velocity ions is perhaps the most dramatic demonstration to date of the apparent validity of the concept of total projectile kinetic energy scaling.

IV. Discussion

To help understand the experimental results, we compare them to numerical simulations of the reactions using the intranuclear cascade model of Yariv and Fraenkel[11]. Previous investigations[3,12] have shown that this model does satisfactorily predict the isobaric yield distributions in the interaction of relativistic light heavy ions (C,Ne) with heavy targets (Ta, Au, U). The version of this model we are using has been described previously[11,12] as has the modified version of the DFF computer code used to calculate the primary fragment deexcitation by particle emission and/or fission. The discussion that follows is based upon ∿1000 cascade events per reaction and ten de-excitation cascades per primary fragment cascade event. The calculations were performed using a VAX 8200 computer.

The isobaric yield distributions for the reaction of 400 MeV/nucleon ^{20}Ne and 150 MeV/nucleon ^{139}La with ^{197}Au predicted by the intranuclear cascade model are compared with the experimental data in Figure 4. The model reproduces the experimental curves reasonably well, giving the correct general magnitude and shape of the distributions. Total kinetic energy scaling of fragment yields thus may be a "conventional" phenomenon in that it is described by the relativistic classical mechanics of the intranuclear

cascade model. (It should be noted nonetheless, that as described previously[3], the charge distributions, particularly of the near-target residues, are not predicted correctly or are the yields of the intermediate mass fragments).

We examined the primary product distributions predicted by this model in hopes of gaining insight into the physics involved in this total kinetic energy scaling. In Figure 5, we show the predicted excitation energy and fragment yield distributions as a function of fragment mass number for the reaction of 150 MeV/nucleon ^{139}La and 400 MeV/nucleon ^{20}Ne with ^{197}Au. While the yield distributions are somewhat similar, the excitation energy distributions are not, although the regions of maximum discrepancy involve predicted excitation energies that may be physically unreasonable, particularly if there is a limiting temperature of nuclear matter[13], beyond which multifragmentation occurs. Apparently the preponderence of events (in the model) occur for very peripheral reactions in which the differences between the two reactions are not so great.

This result led us to speculate that total projectile kinetic energy scaling was due to a combination of two effects that approximately cancel one another. For collisions of two different projectiles of the same total kinetic energy with a given target nucleus at a given impact parameter, the collision of the larger projectile with the target nucleus leads to: (a) more projectile nucleons being transferred to the target nucleus (due to the greater overlap volume between projectile and target nuclei) and (b) a lower excitation energy per transferred nucleon (due to the lower energy/nucleon of the larger projectile). Effects (a) and (b) might cancel each other. To test this speculation numerically, we calculated, using the intranuclear cascade model, the average excitation energy given to the target nucleus and the average number of projectile nucleons transferred to the target nucleus for a series of reactions involving ^{12}C, ^{20}Ne, ^{40}Ar,

^{86}Kr and ^{139}La projectiles with total kinetic energy of 21 GeV with ^{197}Au (figure 6). The results of this calculation indicate the similarity of the excitation energies in the reactions induced by the lighter projectiles (C, Ne) in agreement with previous studies "establishing the validity" of total projectile kinetic energy scaling. Also the calculations indicate, as discussed previously, the approximate equivalence of the transferred excitation energy in the ^{139}La + ^{197}Au reaction with the ^{20}Ne + ^{197}Au reaction. The effect in these three cases (C, Ne, La) seems to be in accord with our speculation in that the number of transferred projectile nucleons is increasing while the average excitation energy remains roughly constant. But the calculations for the ^{40}Ar + ^{197}Au and the ^{80}Kr + ^{197}Au reactions do not indicate a pattern of total kinetic energy scaling in that the average target nucleus excitation energy is substantially different than that predicted for the C, Ne and La induced reactions. If the calculations are correctly simulating the reactions, then the similarity of the results between the ^{20}Ne + ^{197}Au and the ^{139}La + ^{197}Au reactions is a fluke and total projectile kinetic energy scaling is not a generally valid concept. It would be interesting to make appropriate measurements of the ^{40}Ar + ^{197}Au reaction to see if the effects predicted by the cascade model occur.

V. Conclusions

We have shown the near-equivalence of the target fragment mass yield distributions for the reaction of 150 MeV/nucleon ^{139}La (20.8 GeV) with ^{197}Au and the distributions representing limiting fragmentation (such as the reaction of 8 GeV ^{20}Ne with ^{197}Au). This result apparently is an extreme example of total projectile kinetic energy scaling. We find this scaling is apparently a result of "conventional" physics in that

it is predicted by the intranuclear cascade model although that model may indicate a limited validity of this scaling.

We find a substantial cross section for the $^{197}Au(^{139}La,X)\ ^{196}Au$ reaction of (765±48 mb). We deduce a value of the electromagnetic dissociation cross section of 447 mb, a value substantially below the estimates of the Winther-Alder theory.

VI. Acknowledgements

The authors wish to acknowledge the operations staff of the LBL Bevalac for providing excellent beams of ^{139}La and P.J. Siemens for valuable discussions. This work was supported in part by the U.S. Department of Energy under Contract Nos. DE-AM06-76RL02227, Task Agreement No. DE-AT06-76ER70035 and DE-AC03-76SF00098 and the Swedish Natural Sciences Research Council.

References

1. For a review of target fragmentation phenomena, see E.M. Friedlander and H.H. Heckman, in Treatise on Heavy Ion Nuclear Science, Vol. 4, D.A. Bromley, ed. (Plenum, New York, 1985) p. 403.
2. J. Benecke, T.T. Chou, C. N. Yang, and E. Yen, Phys. Rev. 188, 2159 (1969).
3. D.J. Morrissey, W. Loveland, M. de Saint-Simon, and G.T. Seaborg, Phys. Rev. C21, 1783 (1980).
4. J.V. Kratz, J.O. Liljenzin, A. Norris, and G.T. Seaborg, Inorg. Nucl. Chem. Lett. 10, 951 (1974).
5. D.J. Morrissey, D. Lee, R.J. Otto, and G.T. Seaborg, Nucl. Instr. Meth. 158, 499 (1978).
6. M.T. Mercier, J.C. Hill, F.K. Wohn, and A.R. Smith, Phys. Rev. Lett. 52, 898 (1984).

7. A Winther and K. Alder, Nucl. Phys. A319, 518 (1979).

8. S.B. Kaufman, E.P. Steinberg, B.D. Wilkins, and D.J. Henderson, Phys. Rev. C22, 1897 (1980).

9. S.B. Kaufman, and E.P. Steinberg, Phys. Rev. C22, 167 (1980).

10. W. Loveland, K. Aleklett, P.L. McGaughey, K.J. Moody, R.M. McFarland, R.H. Kraus, Jr. and G.T. Seaborg, Lawrence Berkeley Laboratory Report LBL-16280, 1983.

11. Y. Yariv and Z. Fraenkel, Phys. Rev. C20, 2227 (1979).

12. P.L. McGaughey, W. Loveland, D.J. Morrissey, K. Aleklett, and G.T. Seaborg, Phys. Rev. C31, 896 (1985).

13. S. Levit, in Proc. Int'l Nucl. Phys. Conf., Harrogate, J.L. Durell, J.M. Irvine, and G.C. Morrison, eds. (Institute of Physics, Bristol, 1987) p. 227.

TABLE I.

Formation cross sections (mb) of nuclides formed by the reaction of 150 A MeV ^{139}La with ^{197}Au. Independent yields are indicated by (I)

Nuclide	Cross Section	Nuclide	Cross Section	Nuclide	Cross Section	Nuclide	Cross Section
^{24}Na	63.6 ± 5.5	^{100}Pd	3.0 ± 0.8	^{147}Gd	19.4 ± 2.0	^{183}Os	29.2 ± 2.9
^{28}Mg	13.4 ± 0.9	$^{101}Rh^{m}$	13.5 ± 1.0	^{149}Gd	24.9 ± 2.5	$^{183}Os^{m}$	39.3 ± 3.9
^{44}Sc	5.5 ± 0.6	$^{106}Ag^{m}$ (I)	5.9 ± 1.5	^{153}Tb	16.5 ± 0.9	^{184}Ir	36.5 ± 5.1
$^{44}Sc^{m}$ (I)	6.5 ± 1.2	^{109}In	7.8 ± 0.5	^{155}Dy	21.7 ± 2.2	^{185}Os	80.7 ± 4.5
^{47}Sc	16.2 ± 1.0	^{110}In	9.4 ± 0.6	^{157}Dy	25.6 ± 1.3	^{185}Ir	53.9 ± 5.3
^{48}Sc (I)	4.0 ± 0.5	^{111}In	11.2 ± 2.0	^{158}Er	31.9 ± 4.0	^{186}Pt	33.0 ± 3.3
^{48}V	5.5 ± 0.6	^{119}Te	10.7 ± 0.9	^{160}Er	22.0 ± 2.2	^{186A}Ir	34.9 ± 8.9
^{72}As	7.4 ± 1.4	^{121}Te	15.2 ± 0.9	^{161}Er	41.5 ± 2.4	^{186B}Ir	26.6 ± 2.7
^{76}Br	6.9 ± 1.5	^{121}I	15.8 ± 1.1	^{167}Tm	37.0 ± 3.7	^{187}Ir	110 ± 11
^{77}Br	10.3 ± 1.0	^{122}Xe	8.7 ± 1.5	^{169}Yb	26.8 ± 1.5	^{188}Pt	88 ± 4.8
^{81}Rb	6.7 ± 1.4	^{123}Xe	18.2 ± 1.2	^{169}Lu	30.7 ± 6.6	^{191}Pt	107.9 ± 6.7
^{83}Rb	23.2 ± 1.6	^{123}I	24.1 ± 1.6	^{170}Lu	46.0 ± 2.7	^{191}Au	57.0 ± 8.4
^{83}Sr	9.1 ± 1.3	^{127}Xe	14.6 ± 1.9	^{170}Hf	21.3 ± 2.2	^{192}Au	70.7 ± 3.6
^{84}Rb (I)	7.2 ± 1.0	^{127}Cs	20.4 ± 2.4	^{171}Lu	39.3 ± 3.9	^{193}Au	74.5 ± 7.6
^{87}Y	19.1 ± 1.0	^{128}Ba	16.3 ± 1.6	^{171}Hf	37.5 ± 3.8	^{194}Au (I)	123.7 ± 12.4
^{88}Zr	13.6 ± 1.0	^{131}Ba	17.1 ± 1.7	^{173}Hf	29.9 ± 3.0	^{196}Au	765 ± 48
^{89}Zr	14.2 ± 1.2	^{132}Ce	15.1 ± 0.9	^{175}Ta	40.8 ± 4.1	$^{196}Au^{m}$ (I)	10.8 ± 1.1
^{90}Nb	9.7 ± 2.4	^{135}Ce	14.0 ± 1.0	^{176}Ta	51.3 ± 2.6	^{198}Au	23.1 ± 2.3
$^{93}Mo^{m}$ (I)	5.5 ± 1.3	^{145}Eu	20.5 ± 2.1	^{181}Re	51.1 ± 2.9		
^{97}Ru	10.7 ± 0.7	^{147}Eu	24.4 ± 10.2	^{182}Os	42.6 ± 4.3		

TABLE II

Charge Dispersion Parameters

Fragment Mass Number Range	Z_{mp}	C_z
24-48	0.440A + 0.800	0.4
72-90	0.442A + 0.540	0.6
97-119	0.422A + 2.74	0.7
121-135	0.393A + 5.83	0.9
145-160	0.358A + 10.8	1.0
161-176	0.332A + 14.9	0.7
181-188	0.294A + 22.4	0.7
191-194	0.311A + 19.3	0.6

Figure Captions

Figure 1. Ratio of independent yield nuclidic formation cross sections for the interaction of 150 MeV/nucleon ^{139}La with ^{197}Au to those from the reaction of 400 MeV/nucleon ^{20}Ne with ^{197}Au. The solid line shows the average value of the ratio.

Figure 2. The estimated independent yield distributions from the reaction of 150 MeV/nucleon ^{139}La with ^{197}Au. The plotted points are the experimental values and the solid lines are the fitted Gaussian charge distributions.

Figure 3. Isobaric yield distributions for the fragmentation of ^{197}Au by (a) 150 MeV/nucleon ^{139}La, this work, solid points; (b) 200 MeV protons[9], dotted line; (c) 400 MeV/nucleon ^{20}Ne[3], dashed line; (d) 86 MeV/nucleon ^{12}C[10], solid line.

Figure 4. The isobaric yield distributions predicted by the intranuclear cascade model (open bars) are compared to the experimental data (solid line) for the reaction of a) 8 GeV ^{20}Ne and b) 20.8 GeV ^{139}La with ^{197}Au.

Figure 5. The predicted primary fragment excitation energy and yield distributions for the reaction of 20.8 GeV ^{139}La (open bars) and 8 GeV ^{20}Ne (solid bars) with Au^{197}.

Figure 6. (a)The predicted average target nucleus excitation energy and (b)the average number of projectile nucleons transferred to the target nucleus in a series of reactions of 21 GeV ^{12}C, ^{20}Ne, ^{40}Ar, ^{86}Kr and ^{139}La with ^{197}Au.

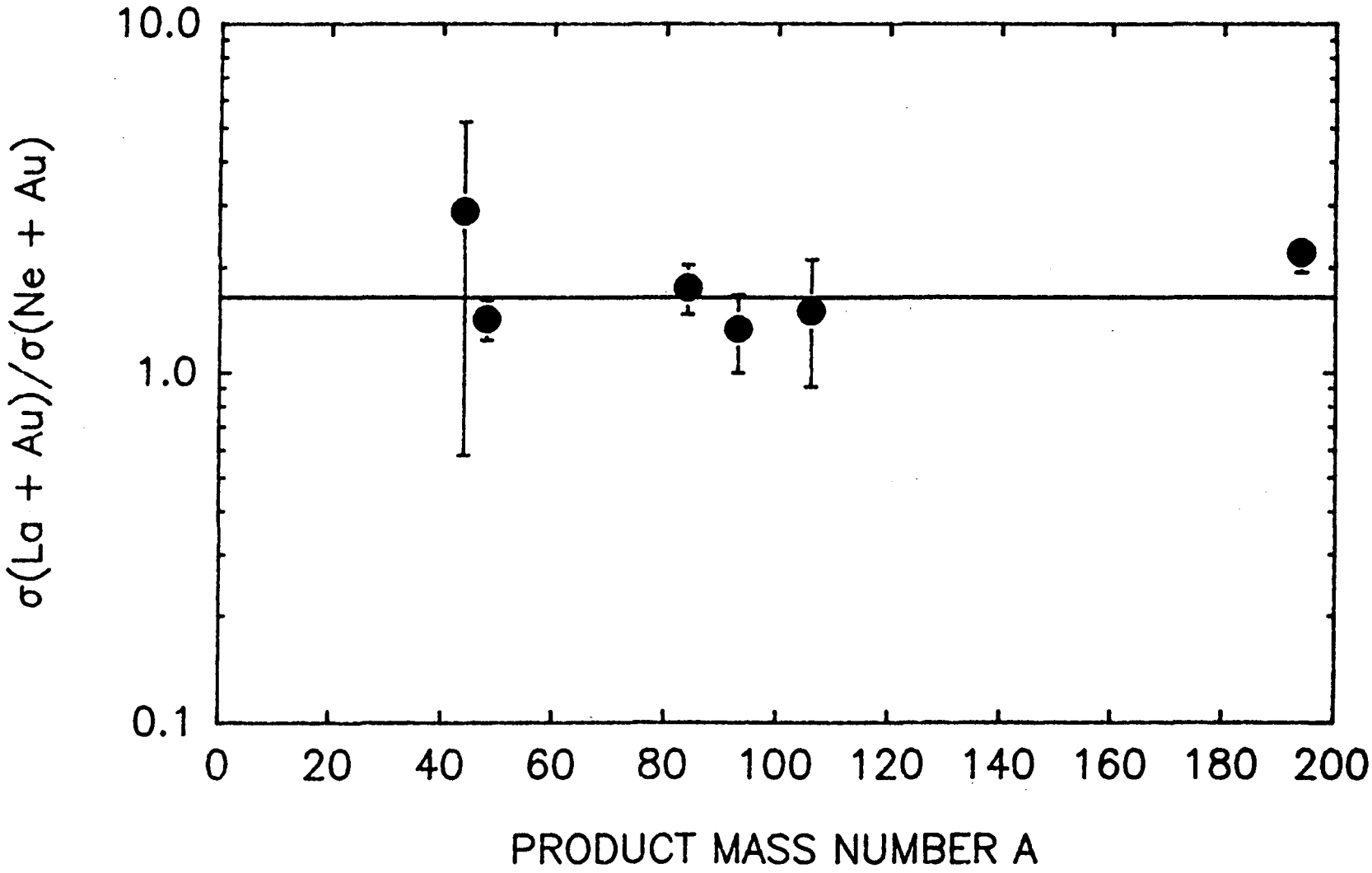
10.0
1.0
0.1
σ(La + Au)/σ(Ne + Au)
0
20
40
60
80
100
120
140
160
180
200
PRODUCT MASS NUMBER A

Fig. 1

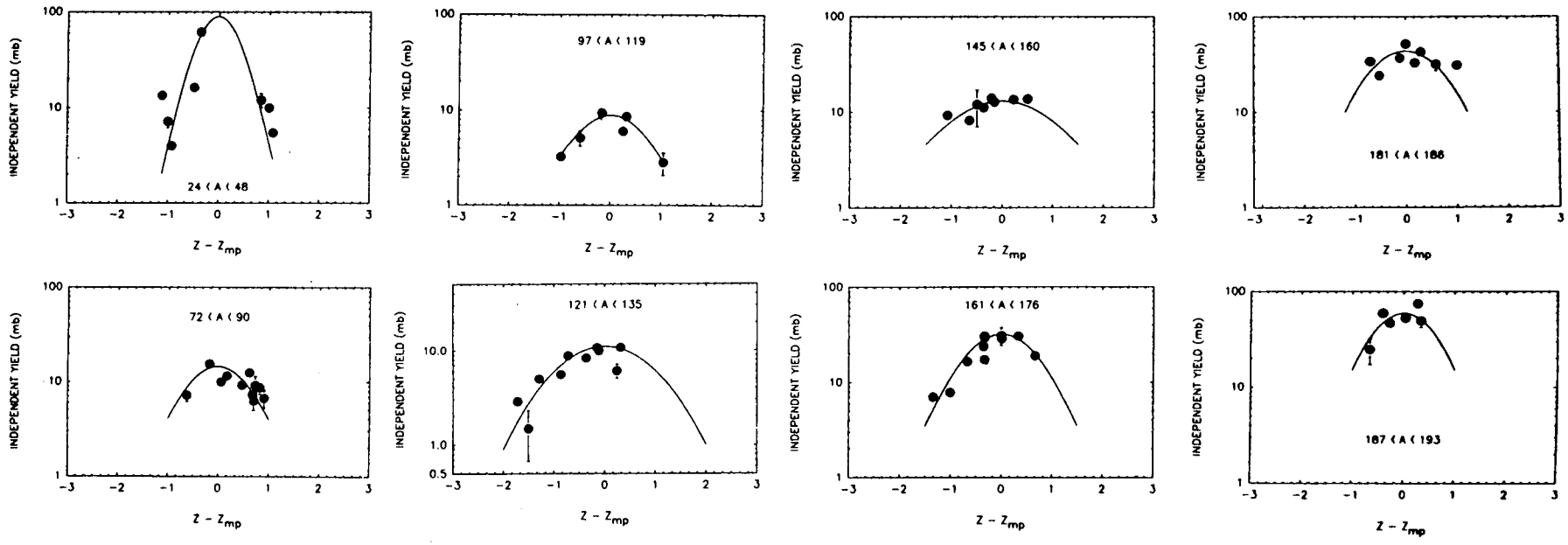
24 < A < 48
97 < A < 119
145 < A < 160
181 < A < 186
72 < A < 90
121 < A < 135
161 < A < 176
187 < A < 193
INDEPENDENT YIELD (mb)
Z - Z_mp

Fig. 2

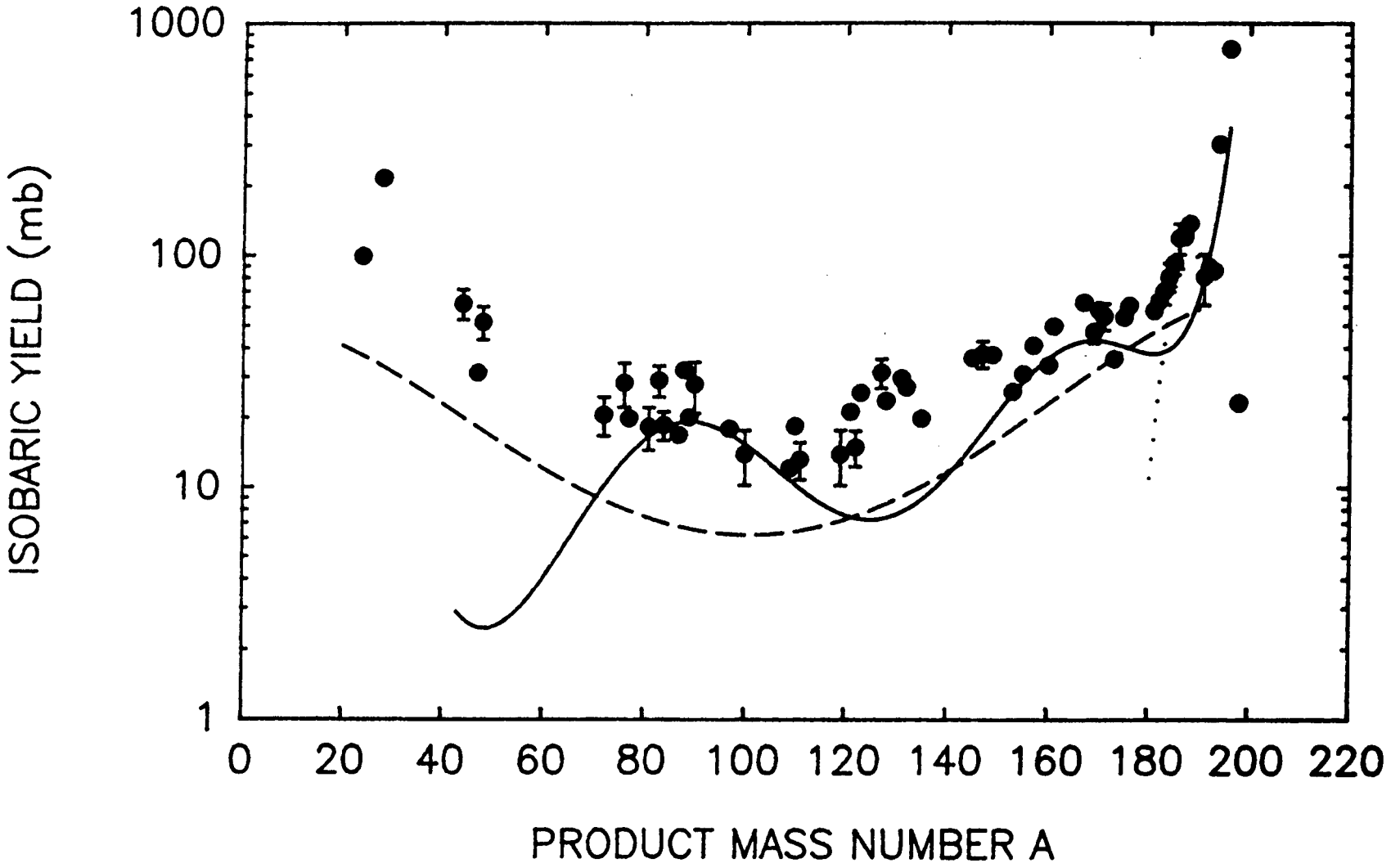
1000
100
10
1
ISOBARIC YIELD (mb)
0
20
40
60
80
100
120
140
160
180
200
220
PRODUCT MASS NUMBER A

Fig. 3

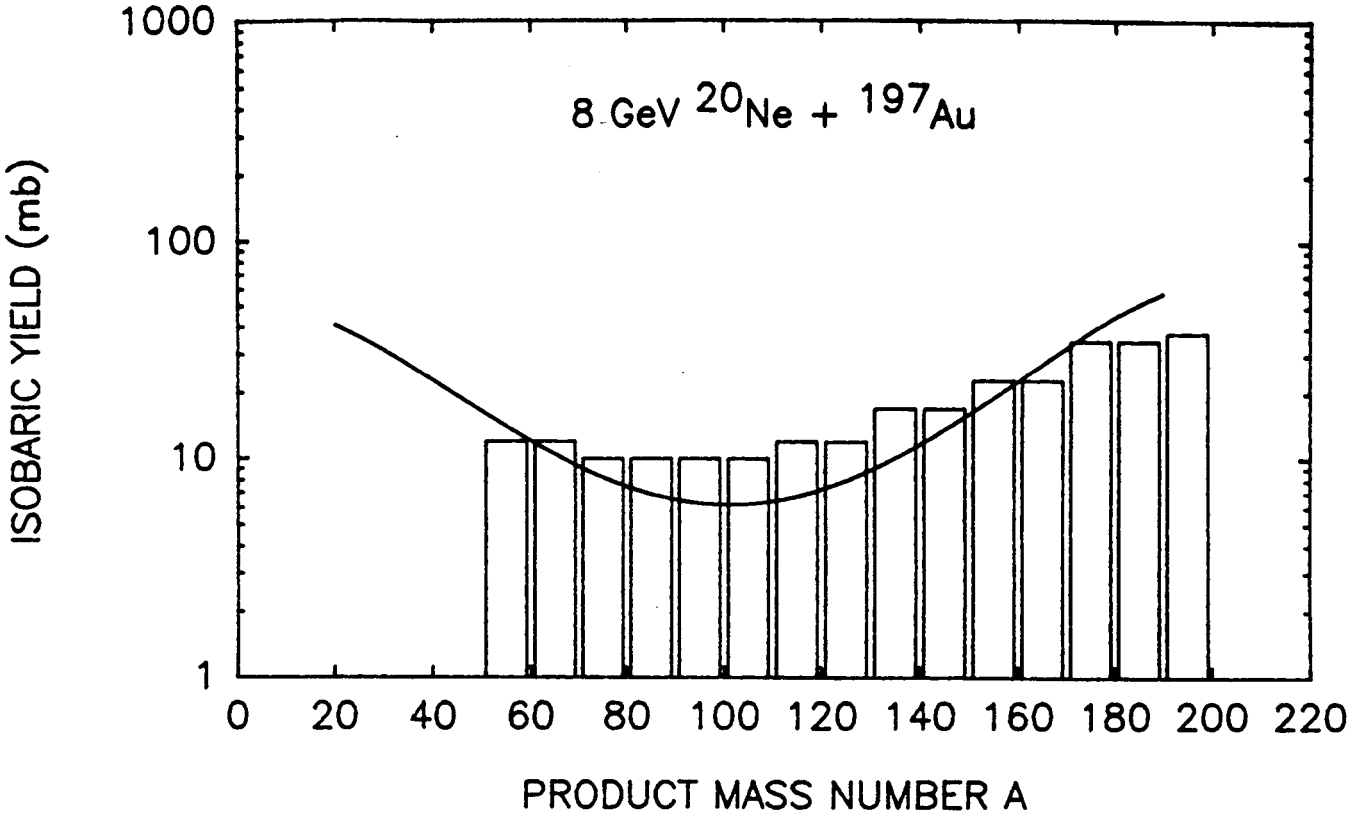
8 GeV ^{20}Ne + ^{197}Au
ISOBARIC YIELD (mb)
1000
100
10
1
0 20 40 60 80 100 120 140 160 180 200 220
PRODUCT MASS NUMBER A

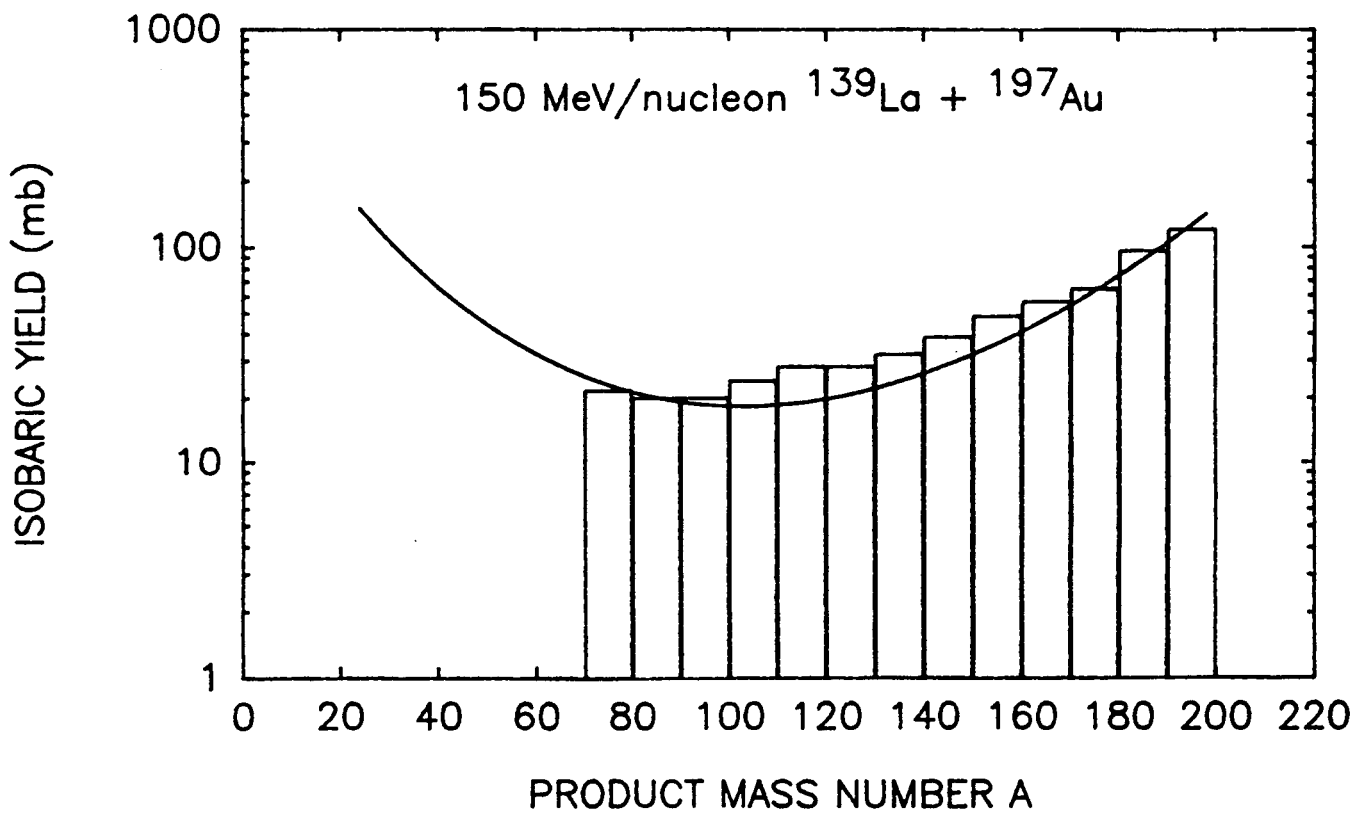
150 MeV/nucleon ^{139}La + ^{197}Au
ISOBARIC YIELD (mb)
1000
100
10
1
0 20 40 60 80 100 120 140 160 180 200 220
PRODUCT MASS NUMBER A

Fig. 4

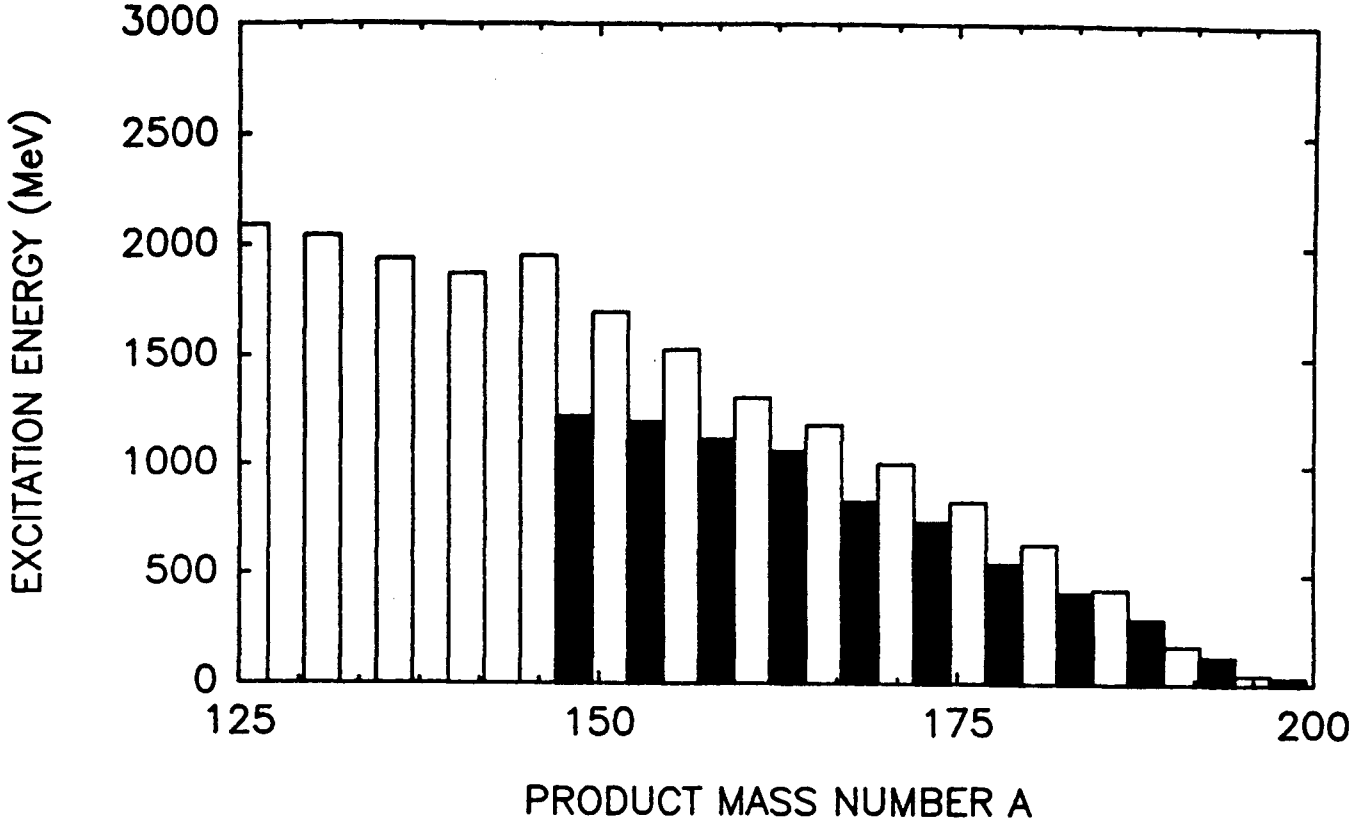
3000
2500
2000
1500
1000
500
0
EXCITATION ENERGY (MeV)
125
150
175
200
PRODUCT MASS NUMBER A

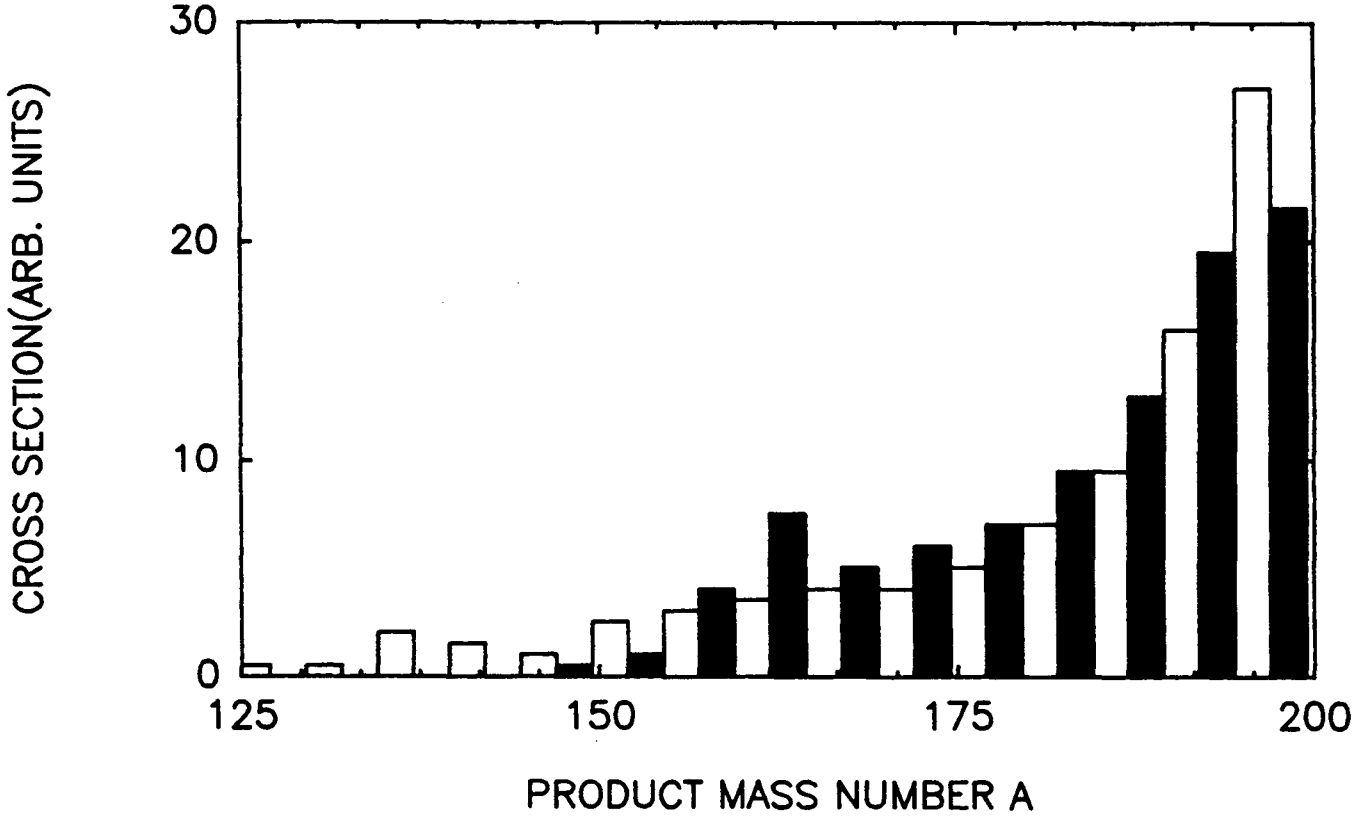
30
20
10
0
CROSS SECTION(ARB. UNITS)
125
150
175
200
PRODUCT MASS NUMBER A

Fig. 5

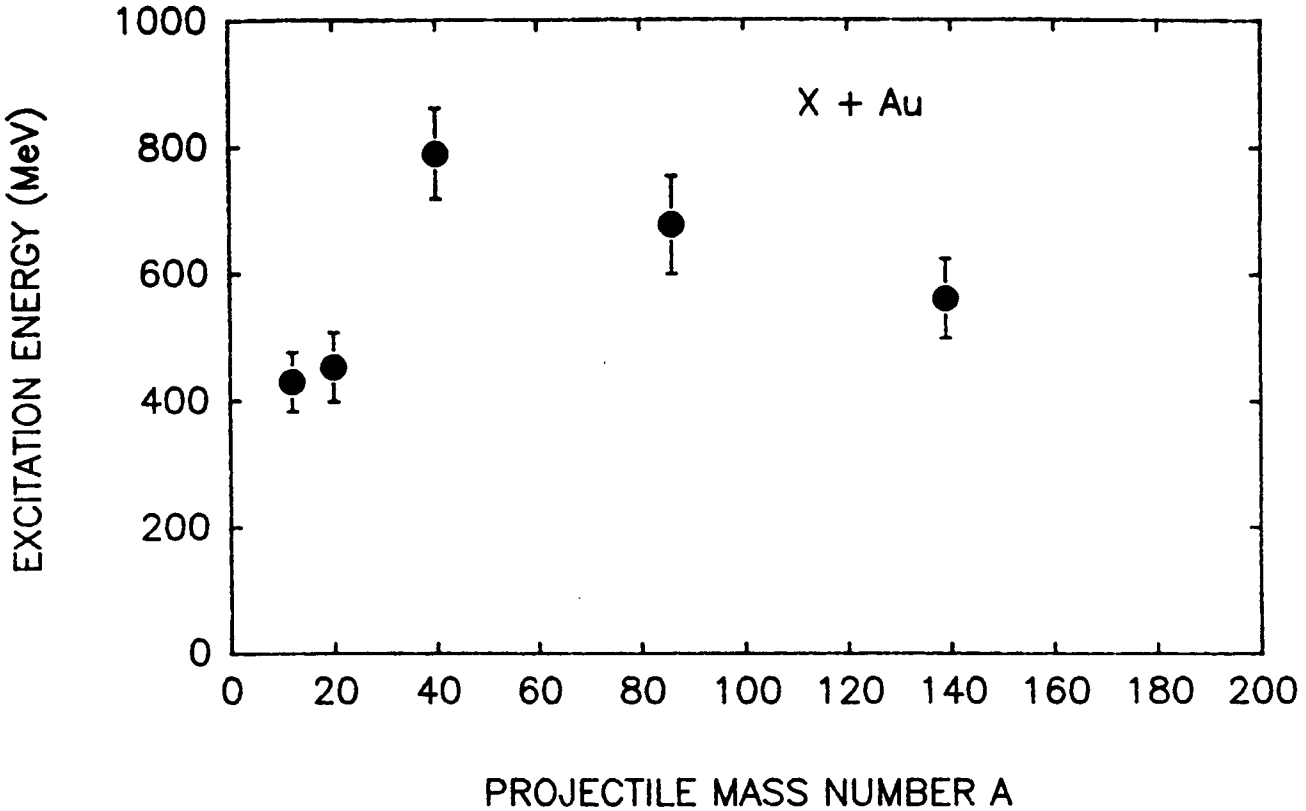
EXCITATION ENERGY (MeV)
1000
800
600
400
200
0
X + Au
0
20
40
60
80
100
120
140
160
180
200
PROJECTILE MASS NUMBER A

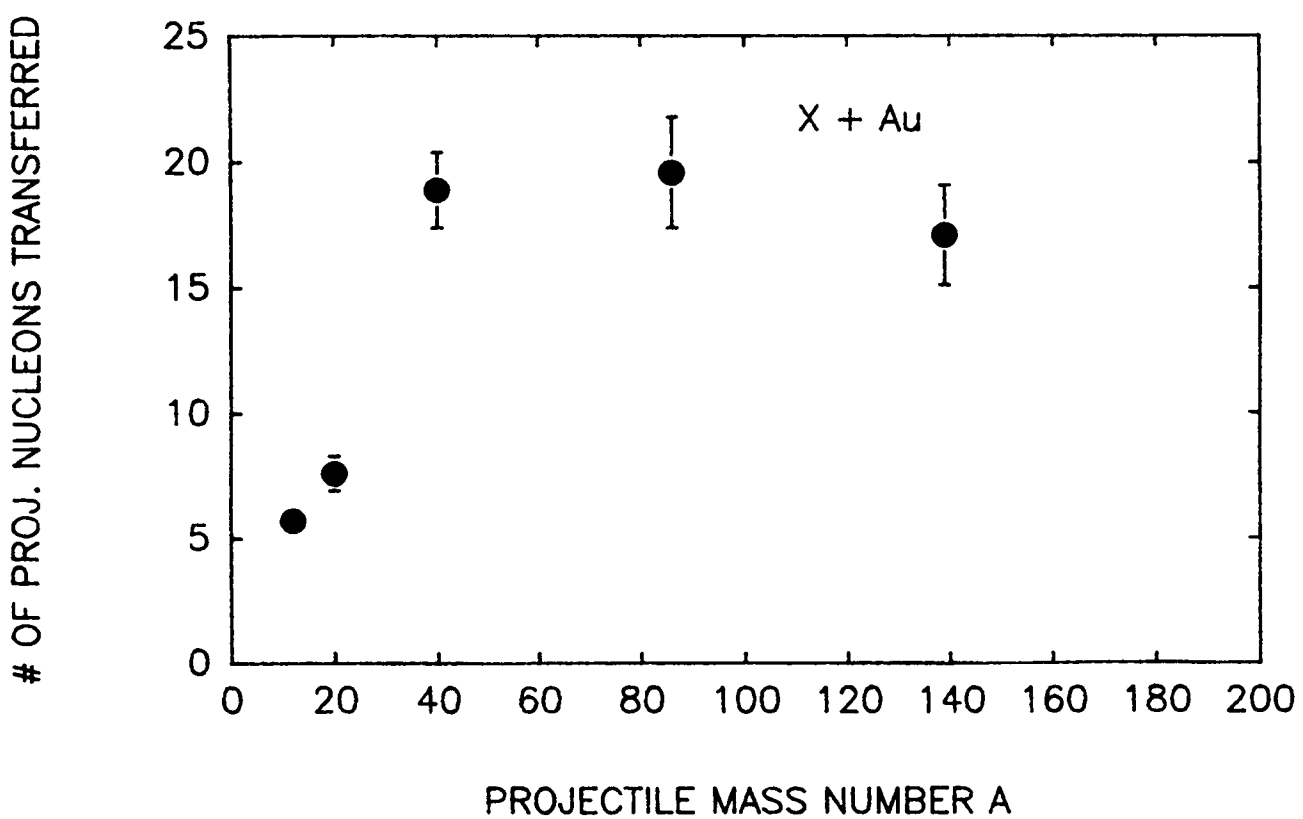
OF PROJ. NUCLEONS TRANSFERRED
25
20
15
10
5
0
X + Au
0
20
40
60
80
100
120
140
160
180
200
PROJECTILE MASS NUMBER A

Fig. 6

LAWRENCE BERKELEY LABORATORY
TECHNICAL INFORMATION DEPARTMENT
UNIVERSITY OF CALIFORNIA
BERKELEY, CALIFORNIA 94720